Kidney International, Vol. 53 (1998), pp. 100–111

CELL BIOLOGY - IMMUNOLOGY - PATHOLOGY

Intracellular targets in heme protein-induced renal injury

KARL A. NATH, JOSEPH P. GRANDE, ANTHONY J. CROATT, SCOTT LIKELY, ROBERT P. HEBBEL, and HELEN ENRIGHT

Nephrology Research Unit and Department of Medicine and Pathology, Mayo Clinic/Foundation, Rochester, and Department of Medicine, University of Minnesota, Minneapolis, Minnesota, USA

Intracellular targets in heme protein-induced renal injury. We examined two potential intracellular targets in the glycerol model of acute renal failure, namely, the mitochondrion and the nucleus. Within three hours, alterations in mitochondrial function are already apparent. With either glutamate/malate or succinate/rotenone, state 3 and uncoupled respirations were decreased at three hours, and at 24 hours, such decrements were quite pronounced; in the presence of glutamate/malate, state 2 respiration was also depressed at 24 hours, while with succinate/rotenone state 2 was increased. Marked ultrastructural changes were observed in mitochondria studied at three hours, including the novel finding of degenerate mitochondria in autophagic vacuoles. Since the heme content in mitochondria was increased some tenfold within three hours, mitochondrial function was studied after exposure to concentrations of heme that reproduced such contents of heme: mitochondria initially displayed increased respiration, and subsequently, a persistent decline in oxygen consumption until oxygen consumption was virtually undetectable. With higher concentrations of heme, the early increase in oxygen consumption was blunted and the progressive decline in oxygen consumption was hastened. The antioxidant iron chelator, deferoxamine, prevented the early rise in oxygen consumption but did not prevent or delay the subsequent decline. We also assessed nuclear damage as a potential lesion in the glycerol model. DNA laddering was not observed at any time point. At 3 and 24 hours there was DNA injury by the TUNEL technique in the distal nephron but not in the proximal nephron. The 8-hydroxydeoxyguanosine/deoxyguanosine content was increased in the glycerol kidneys at 24 hours but not at three hours. At neither time point was evidence of apoptosis observed by light or electron microscopy. In studies undertaken in cell culture models, heme, at concentrations of 10 μM, failed to evince any such changes in LLC-PK_1 cells, a cell line from the proximal tubule, or in MDCK cells, a cell line derived from the distal tubule. At concentrations of 50 μM, heme induced approximately 20% positivity in MDCK cells but none in LLC-PK_1 cells by the TUNEL technique. We conclude that mitochondria and nuclei are prominent targets for injury in the glycerol model of acute renal failure. The presence of TUNEL-positive cells in the distal nephron but not at proximal sites *in vivo* underscores the increasing appreciation of the distinct responses of these nephron sites to nephrotoxic insults.

The intramuscular administration of hypertonic glycerol induces myolysis and hemolysis and affords a faithful, widely utilized model of heme protein-induced renal injury [1, 2]. Studies using this model have contributed substantially to the recognition that heme protein-induced renal injury represents the integrated effects of three major pathophysiologic mechanisms: renal vasoconstriction, direct cytotoxicity, and cast formation [1, 2]. The biochemical underpinnings of renal injury so induced have also received much attention, and in this regard, there is persuasive evidence incriminating oxidative stress and the catalytic effect of redox-active iron as important mechanisms for such injury [1, 3–5].

In contrast to such delineation of the pathophysiologic and biochemical pathways involved in this form of acute renal injury, there is a paucity of information on the cell biology of renal tubular epithelial cell injury in this model: namely, the specific intracellular targets critically damaged in the evolution of cell injury in this setting are largely unidentified, as is the contribution of such organelle dysfunction to the loss of cellular vitality. The present study examines intracellular targets that may be injured in this model, focusing on two such targets, the mitochondrion and the nucleus. The rationale for examining the mitochondrion stems from the recognition of the importance of injury to this organelle, in general, as a contributor to cell injury in other forms of toxic injury [6, 7], while recent studies of myohemoglobinuria, in particular, have demonstrated free radical production by mitochondria as an initiator of lipid peroxidation [8]; together, these studies raise the possibility that this organelle may represent a contributor as well as a target of injury in this disease model. Moreover, interest in the mitochondrion has noticeably resurfaced [9] as it is currently and increasingly appreciated that mitochondrial dysfunction, and in particular, the appearance of the mitochondrial permeability transition [9], is present in diverse states that induce or are attended by programmed cell death. Such mitochondrial dysfunction may represent a key step in the cascade of cellular events leading to programmed cell death. Mitochondrial injury is thus relevant to apoptotic as well as necrotic death.

Nuclear events and changes in the course of cellular demise are also the focus of much attention. Endonuclease activation is commonly observed in a number of models of cell death, and in certain instances, even in the absence of classic morphologic changes of apoptosis [10–12]. In view of the importance of oxidative stress in this model [1, 3–5], and the vulnerability of the nucleus to oxidative stress [10], we posited that this cellular site may also be the target of injury. Employing multiple indices—electrophoretic analysis of DNA, fragmentation of DNA using the terminal deoxynucleotidyl transferase (TUNEL) assay, the 8-hydroxdeoxyguanosine assay and electron microscopic analysis—we assessed DNA injury in conjunction with studies of

Key words: heme protein, renal injury, acute renal failure, nuclear damage, mitochondrial injury.

Received for publication April 30, 1997
and in revised form August 12, 1997
Accepted for publication August 13, 1997

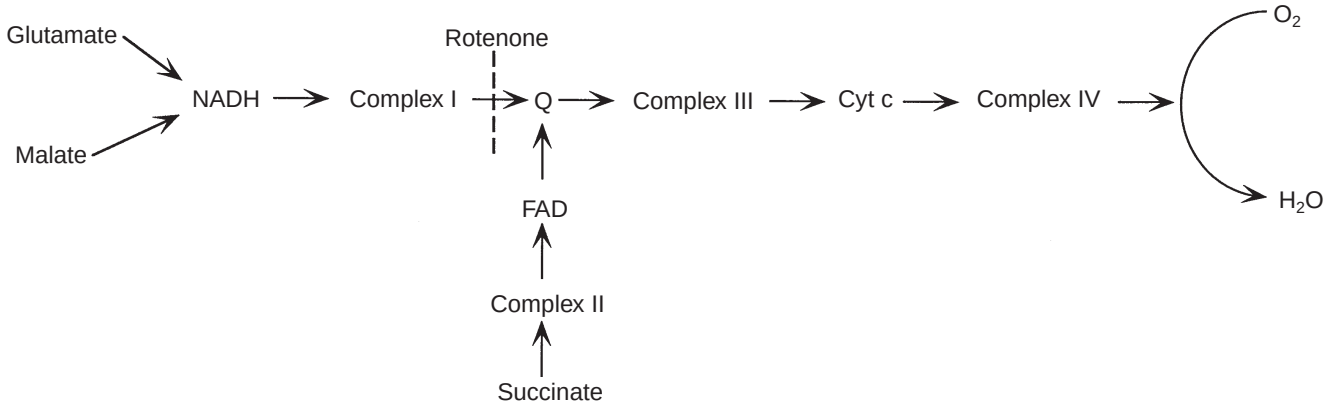

Fig. 1. Scheme showing electron transport chain in the mitochondrion.

mitochondrial function. We observed marked mitochondrial dysfunction within hours of inducing the glycerol model. DNA injury, detectable principally by the deoxynucleotidyl transferase assay, was observed in the distal nephron. Some of the observed changes are inducible by heme, thus raising the possibility that this component of heme proteins may be a contributor to organellar injury that evolves in this disease state.

METHODS

Oxygen consumption by mitochondria

The glycerol model was induced by the injection of a 50% solution of glycerol (10 ml/kg body wt, half the dose into each thigh muscle) into rats that were deprived of water overnight, but allowed to feed *ad libitum* [13]. Mitochondria were extracted and oxygen consumption was determined using a Clark electrode as described by Lemmi et al [14], and as employed previously in studies from our laboratory [15]. Malate (10 mM)/glutamate (10 mM) or succinate (10 mM)/rotenone (5 μM) were used as substrates. State 2 mitochondrial respiration was determined in the basal state following the injection of the mitochondria into the chamber; State 3 respiration was determined as ADP (200 μM)-stimulated respiration, and State 4 respiration was determined after the utilization of ADP. Uncoupling was induced by dinitrophenol, 100 μM. The respiratory control ratio (RCR) was calculated as State 3/State 4, the acceptor control ratio (ACR) as State 3/State 2 and the P/O ratio represented ADP utilized/oxygen consumed. Figure 1 shows a simplified schema for the mitochondrial electron transport chain.

In studies involving heme, a stock solution of hemin (iron protoporphyrin IX) chloride dissolved in 0.1 N potassium hydroxide was freshly prepared with each experiment and diluted to the stated concentration. For example, in studies of oxygen consumption, the diluent used was the oxygen consumption buffer, while in studies of cytotoxicity the diluent was Hank's balanced salt solution.

Measurement of 8-hydroxydeoxyguanosine

The formation of 8-hydroxydeoxyguanosine (8OHdG) in DNA, a marker of DNA oxidative injury, was measured as described by Floyd et al [16], and as previously performed by our laboratory [17, 18], in DNA isolated from kidneys of rats subjected to hypertonic glycerol and from the kidneys of control rats. DNA was extracted using phenol and chloroform, ethanol-precipitated, resuspended in 10 mM Tris/1 mM EDTA, pH 7.4 and extensively digested with the following enzymes: DNAse 1 (bovine pancreas; Calbiochem), endonuclease *Neurospora crassa* (Boehringer Mannheim), phosphodiesterase snake venom *Crotalus duriss* (Boehringer Mannheim) and alkaline phosphatase (calf intestine; Calbiochem). The amounts of deoxyguanosine (dG) and of 8OHdG in the resulting deoxynucleoside mixture were detected using a high-performance liquid chromatograph (Hewlett Packard 1090LC) with in-line ultraviolet and electrochemical (Hewlett Packard EC 1049A) detectors, respectively. The analytical column used was a C18 5 μm ODS Hypersil 2.1 $\times$ 100 mm column (Hewlett-Packard #799160D-522 EA). The mobile phase was 2.8% methanol containing 4 mM citric acid, 8 mM sodium acetate (anhydrous), 10 mM sodium hydroxide, 0.067% glacial acetic acid, flow rate 0.3 ml/min. Results are expressed as 8OHdG/10^5dG. Deoxyguanosine was measured in pmolar quantities. The 8OHdG standard was a kind gift from Dr. Robert Floyd and the dG standard was purchased from Sigma Chemical Company.

We studied this index in the kidney at three hours and 24 hours after the administration of hypertonic glycerol (10 ml/kg body wt). Since we hypothesized that this index is increased in the glycerol kidney, the protocol at three hours included an antioxidant manipulation, namely, sodium pyruvate, which we have shown previously decreases this index of DNA oxidative injury [18]. We thus studied the effect of sodium pyruvate or sodium chloride in rats subjected to glycerol or control animals. Rats were anesthetized with Inactin and a tracheal catheter and jugular venous catheter placed. A bolus of 8% sodium pyruvate or equimolar sodium chloride (0.5% body wt over 15 min) was infused over 15 minutes followed by 1 ml/hr sustaining infusions for three hours. At the time of initiating these infusions, 50% glycerol was injected, and three hours thereafter the kidneys were harvested. In a separate study rats were injected with 50% glycerol (10 ml/kg/body wt) and 24 hours thereafter kidneys were harvested from these and control rats.

Electrophoresis of DNA

DNA extraction and electrophoresis were carried as previously described in detail in prior publications from our laboratory [17–19]. In brief, Sprague-Dawley rats were anesthetized with ether, and bilateral nephrectomies were performed. Kidneys were

immediately placed in liquid nitrogen and processed for DNA extraction as follows: tissue was macerated immediately, suspended in digestion buffer consisting of 25 mmol/liter EDTA, pH 7.9, 10 mmol/liter Tris, 100 mmol/liter NaCl, and gently homogenized twice (Dounce homogenizer; Fisher Scientific, Pittsburgh, PA, USA). Proteinase K (final concentration 100 μg/ml) and sodium dodecyl sulfate (0.5%) were added, followed by 50 μl/ml of 2-mercaptoethanol. The samples were tightly sealed and incubated at 50°C for three hours. DNA was then extracted by conventional methods by using phenol (freshly-buffered) and chloroform. After ethanol precipitation of DNA, samples were resuspended in Tris-EDTA buffer, treated with ribonuclease, and re-extracted. DNA (10 μg) from each sample was electrophoresed on a 1.5% Nusieve, 0.5% Seakem agarose gel (FMC Bioproducts, Rockford, MD, USA) and visualized under ultraviolet light after ethidium bromide staining.

Detection of DNA fragmentation using the terminal deoxynucleotidyl transferase technique (TUNEL)

Kidneys from rats with glycerol-induced renal failure and control animals were embedded and frozen in O.C.T. freezing medium, and five micron cryosections were cut and mounted on glass slides. These sections were first fixed in 10% neutral buffered formalin for 10 minutes at room temperature then post-fixed in a 2:1 solution of ethanol and glacial acetic acid at −20°C for five minutes. Detection of DNA fragmentation was performed using the Apotag Plus *in situ* Apoptosis Detection Kit (Oncor, Gaithersburg, MD, USA) [20–22]. This kit employs 3′-OH end-extension of fragmented DNA using terminal deoxynucleotidyl transferase (TdT) and a detection system based on an anti-digoxigenin antibody conjugated with peroxidase. The manufacturer's procedure and recommendations were followed with a sham incubation (without TdT) performed for every tissue specimen tested. Additionally, a positive control consisting of a section of normal kidney incubated with 80 U/ml of DNAseI (BMB, Indianapolis, IN, USA) for 10 minutes at room temperature was also performed in all studies. The sections were counterstained using methyl green.

In a similar fashion, DNA fragmentation was assessed in LLC-PK_1 and MDCK cells exposed to heme. Cells were seeded into Lab-Tek Permonox slide chambers (NUNC, Naperville, IL, USA) and grown to near (90%) confluency. After washing the monolayers twice with HBSS, the cells were exposed for three hours to HBSS alone (control) or HBSS containing 10 μM or 50 μM heme. After this exposure the cells were again washed twice with HBSS, fixed with 4% neutral buffered formalin at room temperature, and post-fixed with a 2:1 solution of ethanol and acetic acid at −20°C. After a 10 minutes incubation with proteinase K (20 μg/ml, Gibco/BRL) at room temperature, detection of DNA fragmentation was carried out as described above.

Determination of malondialdehyde in kidney mitochondria

We measured malondialdehyde content in kidney mitochondria by determining the content of thiobarbituric acid reactive substances (TBARS) as previously described from our laboratory [23].

Determination of heme content

We measured heme content in mitochondria by the pyridine-chromogen method as previously described for our laboratory [24].

Structural studies by electron microscopy

Renal tissue was cut into 1 mm cubes, fixed for 24 hours in Trump's fixative (1% glutaraldehyde and 4% formaldehyde in 0.1 M phosphate buffer, pH 7.2) [25] and rinsed for 30 minutes in three changes of 0.1 M phosphate buffer, pH 7.2. Survey sections were cut at 1 μm and stained with toluidine blue. The tissue was post-fixed for one hour in 1% OsO_4 and stained with 2% uranyl acetate for 30 minutes at 60°C. The tissue was dehydrated in progressive concentrations of ethanol and propylene oxide and embedded in Spurr's resin [26]. Thin (90 nm) sections were cut on a Reichert Ultracut E microtome, placed on 200 mesh copper grids, and stained with lead citrate. Micrographs were taken on a JEOL 1200 EXII operating at 60 KV.

Statistical analysis

Data are presented as means ± SEM. For comparisons of two groups involving unpaired data, the unpaired Student's *t*-test was employed. One-way ANOVA was employed for comparisons involving more than two groups and the Student-Newman-Keuls test then applied. Results are considered significant for $P < 0.05$.

RESULTS

Studies of mitochondrial function

Respiration was impaired in mitochondria harvested from the kidney three hours after the administration of glycerol. As shown in Figure 2 at this relatively early time point, mitochondrial respiration, sustained by glutamate and malate, exhibited significant reductions in state 3 respiration and uncoupled respiration without changes in state 2 or state 4 respiration; the RCR, ACR and P/O ratios were all significantly reduced. By 24 hours after the administration of glycerol (Fig. 3, mitochondrial respiration, again sustained by glutamate and malate, was more severely depressed: state 2 respiration was markedly suppressed, and mitochondria failed to respond to ADP or the uncoupling agent, DNP; the ACR was essentially unity. Because no change in oxygen consumption was observed after the addition of ADP, the cessation of state 3 and the commencement of state 4 could not be determined; the determination of state 4 and the calculation of RCR and the P/O ratios were thus not possible. Thus, marked impairment of mitochondrial function, as measured by basal, ADP-driven and uncoupled respiratory rates, was apparent at a time point at which renal failure is established, that is, 24 hours after the administration of glycerol. Impairment in state 3 and uncoupled respiration was discernible even at three hours after the administration of glycerol.

Abnormalities in respiration using succinate and rotenone were also discernible at these two time points. Similar to glutamate and malate, state 3 respiration and uncoupled respiration were diminished, while states 2 and 4 were unchanged in studies undertaken three hours after the administration of glycerol (Fig. 4). However, by 24 hours, basal rates of respiration (state 2) driven by succinate had risen while state 3 and uncoupled respiration were significantly diminished; mitochondrial response to ADP or DNP was again profoundly blunted (Fig. 5). Thus, 24 hours after the administration of glycerol, respiration was significantly increased in the basal state but was largely unresponsive to ADP or to uncoupling agents. That basal mitochondrial respiration in the presence of succinate and rotenone was not impaired, whereas

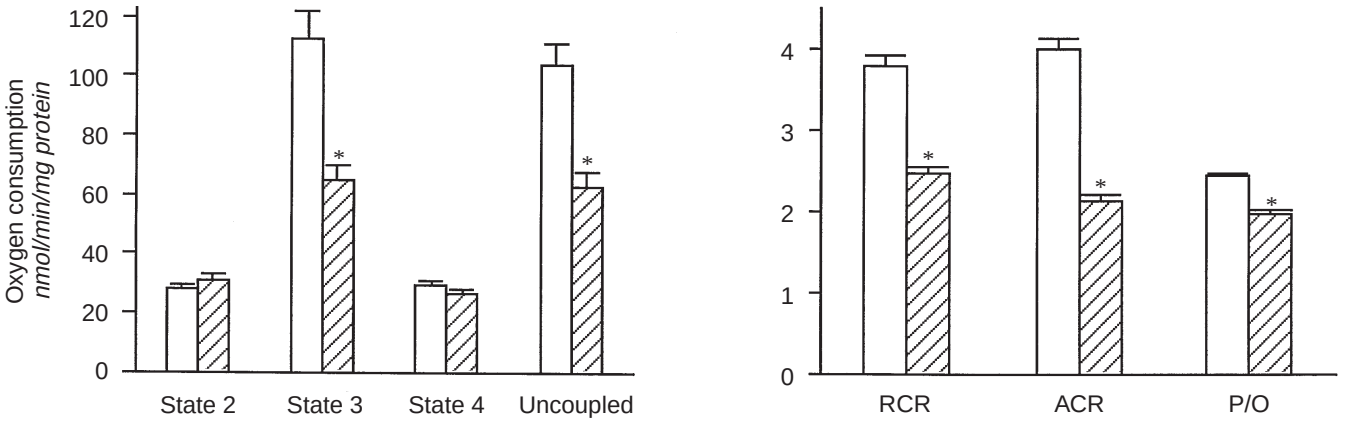

Fig. 2. Respiratory indices in mitochondria studied in the presence of glutamate (10 mM) and malate (10 mM) in rats with glycerol-induced renal injury (▨, $N = 8$) and control rats (□, $N = 9$) studied three hours after the injection of glycerol (*$P < 0.05$).

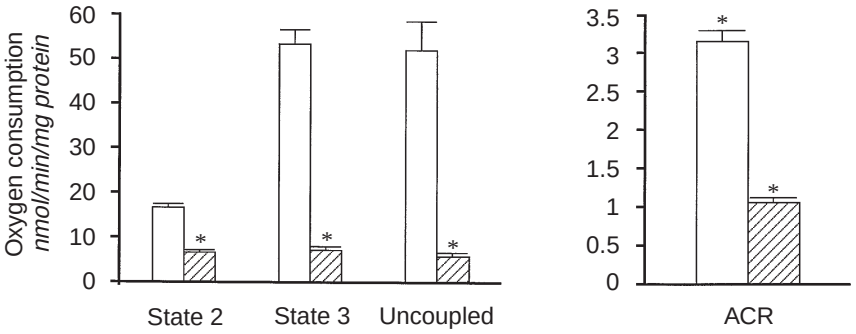

Fig. 3. Respiratory indices in mitochondria studied in the presence of glutamate (10 mM) and malate (10 mM) in glycerol-induced acute renal failure (▨; $N = 5$) and control rats (□, $N = 5$) studied 24 hours after the administration of glycerol (*$P < 0.05$).

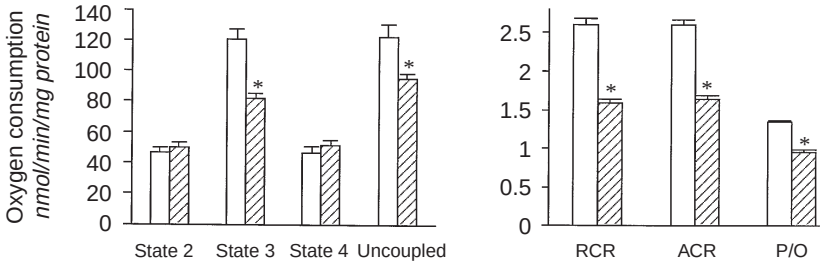

Fig. 4. Respiratory indices in mitochondria studied in the presence of succinate (10 mM)/ rotenone (5 μM) in glycerol-induced acute renal failure (▨, $N = 6$) and control rats (□, $N = 6$) three hours after the administration of glycerol (*$P < 0.05$).

severe reduction in basal mitochondrial respiration in the presence of glutamate and malate was manifest 24 hours after the administration of glycerol, suggests that mitochondrial respiration is impaired, at least in part, at sites at or between the entry of glutamate and malate and Complex 1 (Fig. 1).

To determine if such alterations in mitochondrial function may be due to heme proteins, we exposed mitochondria harvested from normal rats to hemoglobin at different concentrations, 10 and 50 μM. As shown in Table 1, hemoglobin exerted no effect on any of the determined indices of mitochondrial respiration.

Since the endocytotic uptake of hemoglobin in the kidney is followed by the separation of the heme and globin moieties, we considered whether heme would influence mitochondrial function. We measured heme content in mitochondria in the glycerol model at three hours and 24 hours after the administration of glycerol. As shown in Figure 6, heme content was markedly increased at three hours, and remained elevated, although to a lesser degree, at 24 hours after the administration of glycerol. Accompanying this increase in heme were increased amounts of TBARS, the latter representing a marker of oxidative stress (Fig. 7).

We proceeded to study the effects of heme on mitochondrial function in mitochondria harvested from kidneys from normal rats. We employed glutamate and malate as fuel sources since it was with these substrates that the impairment in oxygen consumption was more pronounced in mitochondria studied 24 hours after glycerol-induced renal injury. We exposed mitochondria from intact kidneys to concentrations of heme ranging from 10 to 75

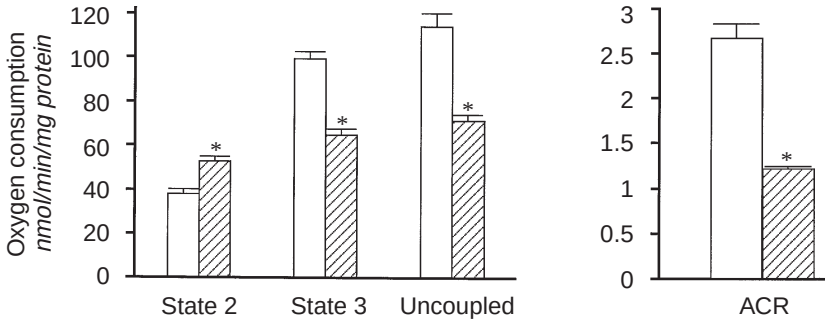

Fig. 5. Respiratory indices in mitochondria studied in the presence of succinate (10 mM)/ rotenone (5 μM) in glycerol-induced acute renal failure (▨, $N = 5$) and control rats (□, $N = 5$) 24 hours after the administration of glycerol (*$P < 0.05$).

Table 1. Effect of hemoglobin at concentrations of 10 and 50 μM on mitochondrial respiration as determined by respiratory rates (nmol/min/mg prot) for state 2 (St 2), state 3 (St 3), state 4 (St 4) and by the RCR and P/O ratios in the presence of glutamate (10 mM) and malate (10 mM)

	St2	St3	St4	RCR	P/O
Control ($N = 4$)	30.8 ± 0.9	115.2 ± 9.5	29.8 ± 1.6	3.9 ± 0.4	2.6 ± 0.1
Hemoglobin, *10 μM* ($N = 3$)	35.3 ± 0.2	107.8 ± 7.6	29.6 ± 1.9	3.6 ± 0.1	2.6 ± 0.1
Hemoglobin, *50 μM* ($N = 3$)	34.9 ± 0.5	117.6 ± 8.7	29.0 ± 1.7	4.1 ± 0.2	2.6 ± 0.1

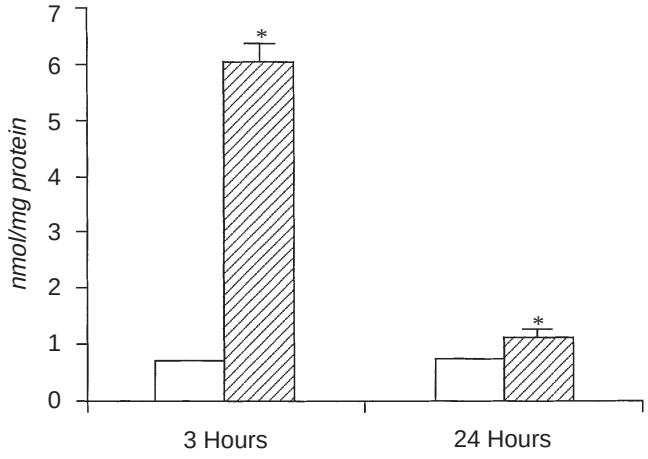

Fig. 6. Mitochondrial heme content hours in glycerol-induced acute renal failure (▨, $N = 6$) and control rats (□, $N = 6$) determined three hours and 24 hours after the administration of glycerol (*$P < 0.01$ vs. control).

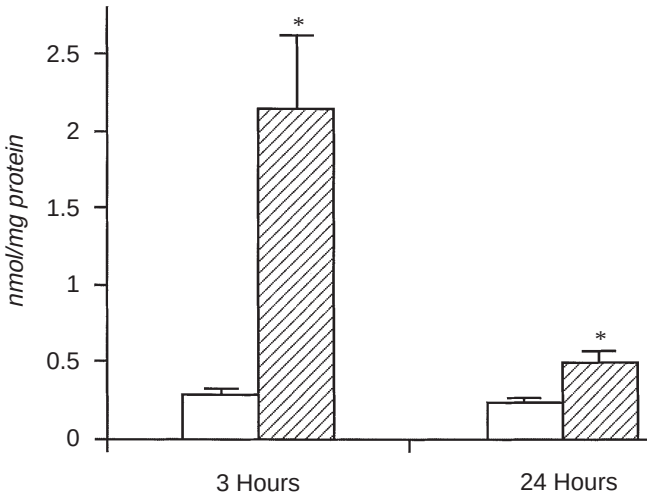

Fig. 7. Mitochondrial TBARS in glycerol-induced acute renal failure (▨, $N = 6$) and control rats (□, $N = 6$) studied 3 and 24 hours after the administration of glycerol (*$P < 0.01$ vs. control).

μM. This range of concentrations was used since exposure of intact mitochondria to a heme concentration of 10 μM reproduced the heme content (6.0 nmol/mg protein) measured in mitochondria harvested from the kidney three hours after the administration of glycerol. As shown in Figure 8, there were dose and time dependent effects of heme on mitochondrial function. Lower doses of heme, such as 10 and 25 μM, initially stimulated mitochondrial respiration. With increasing concentrations of heme, a progressive decline in respiration occurred, and in the case of the highest concentration tested, namely 75 μM, there was a rapid loss of mitochondrial respiration (Fig. 8A). As shown in Figure 8B, at a specific time point, that is, five minutes after exposure to heme, heme at concentrations of 10 μM and 25 μM stimulated mitochondrial respiration whereas 50 μM suppressed mitochondrial respiration. With time, all concentrations of heme employed in the concentration range 10 to 75 μM ultimately impaired mitochondrial respiration, and the lower the dose, the longer the time taken to impair mitochondrial respiration. For example, in the presence of 10 μM heme mitochondrial oxygen consumption was negligible after 40 minutes (*vide infra*), whereas such impairment was observed within 10 minutes with concentrations of 75 μM.

Since heme at a concentration of 10 μM achieves a mitochondrial heme content that mirrors that observed in mitochondria harvested from the glycerol-treated animal, we employed this concentration in further studies of heme-induced alterations of mitochondrial function. We considered the possibility that oxidative stress may contribute to such changes since increased mitochondrial content of TBARS was observed in mitochondria harvested from the glycerol treated animal. To determine the role of oxidative stress in inducing such alterations, we studied the effects of the iron-chelating anti-oxidant, deferoxamine (DFO, 50

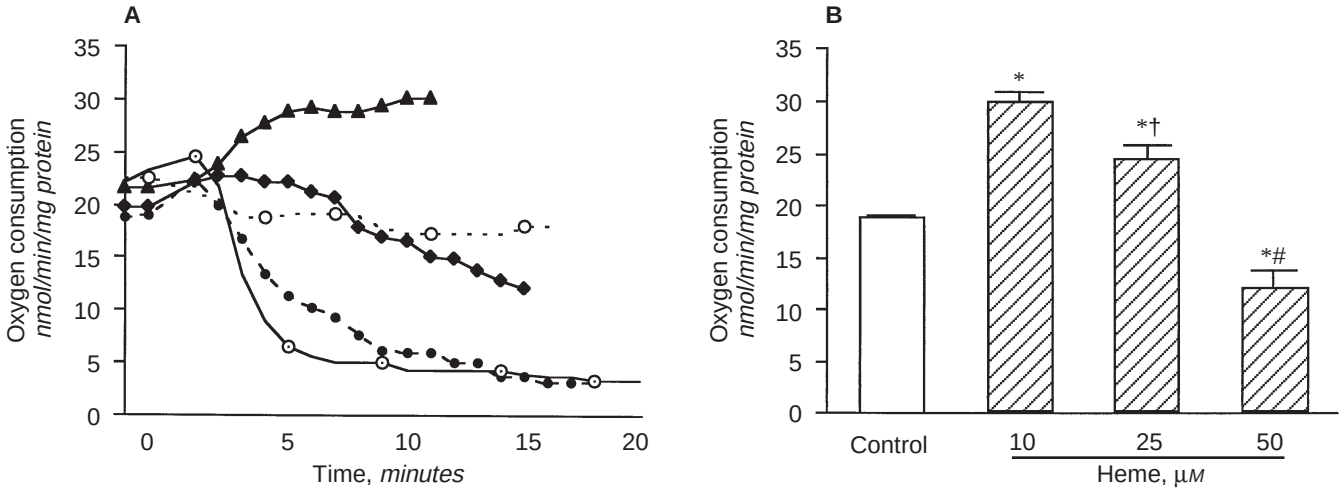

Fig. 8. (*A*) Dose-dependent and time-dependent effects of heme at concentrations of 10 (▲), 25 (♦), 50 (●) and 75 (⊙) μM on mitochondria harvested from healthy rats with intact kidneys; (○), time control mitochondrial respiration in the absence of heme. Each concentration represents the mean of 2 to 4 determinations. (*B*) Effect of specific concentrations of heme, 10, 25 and 50 μM on respiration of mitochondria harvested from healthy rats and determined at five minutes after the exposure to these concentrations of heme. $N = 6$ in each group. *Significantly different from the control. †Significantly different from 10 or 50 μM. #Significantly different from 10 or 25 μM. Oxygen consumption was studied in the presence of glutamate (10 mM) and malate (10 mM).

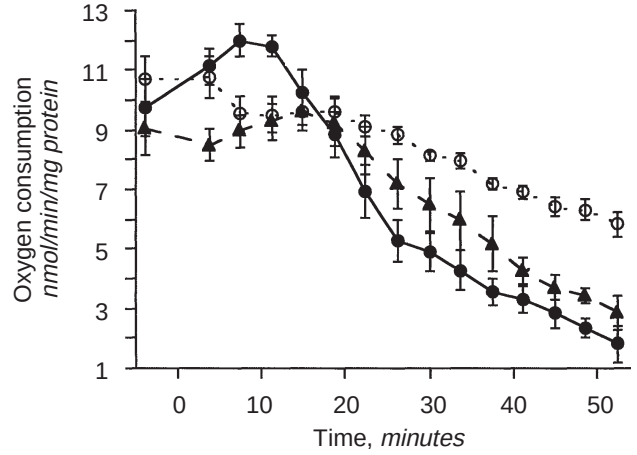

Fig. 9. Effect of deferoxamine on heme-induced alterations of mitochondrial respiration when mitochondria from intact kidneys are exposed to heme (10 μM, ●, $N = 5$) in the absence (○) or presence (▲) of deferoxamine (50 μM). Oxygen consumption was studied in the presence of glutamate (10 mM) and malate (10 mM).

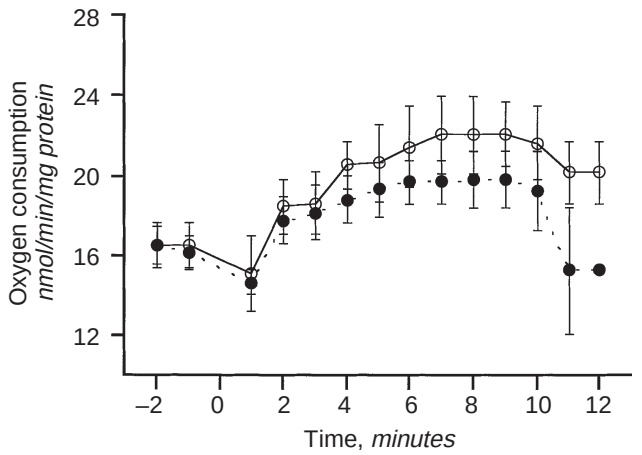

Fig. 10. Effect of BHT on heme-induced alterations of mitochondrial respiration when mitochondria from intact kidneys were exposed to heme (10 μM) in the absence (○, $N = 4$) or presence (●, $N = 4$) of BHT 30 (μM). Oxygen consumption was studied in the presence of glutamate (10 mM) and malate (10 mM).

μM). As shown in Figure 9, DFO prevented the early increase in oxygen consumption induced by heme. However, DFO failed to inhibit the ultimate decline in mitochondrial respiration induced by heme (Fig. 9). We also studied the effect of the antioxidant, butylated hydroxytoluene (BHT; 30 μM). Absolute mitochondrial respiration rates were numerically but not statistically lower in the presence of BHT (Fig. 10). The maximum increment in oxygen consumption induced by heme, 10 μM, however, was significantly less in the presence of BHT, whether expressed as the absolute increment (6.00 ± 0.99 vs. 3.30 ± 0.10 nmol/min/mg protein, $P < 0.05$) or the % increment over basal values (36.4 ± 5.9 vs. 20.1 ± 0.5%, $P < 0.05$). Butylated hydroxytoluene, like DFO, did not inhibit the ultimate decline in mitochondrial respiration induced by heme (data not shown).

Studies of DNA injury

We employed four indices by which to assess DNA damage in the glycerol model. Gel electrophoresis failed to reveal evidence of endonucleosomal cleavage by the laddering pattern at any time point. Measurements of $8OHdG/10^5dG$ in the glycerol model demonstrated that there were no significant differences in this index in the kidney among the four groups studied three hours after the injection of hypertonic glycerol. The sodium chloride-glycerol treated group was not significantly different from the sodium chloride-treated control nor was the pyruvate-treated glycerol group different from the pyruvate-treated control or the sodium chloride-glycerol treated group (Table 2). Thus, at an early time point at which mitochondrial dysfunction was already apparent, no change in this marker of DNA oxidative injury was

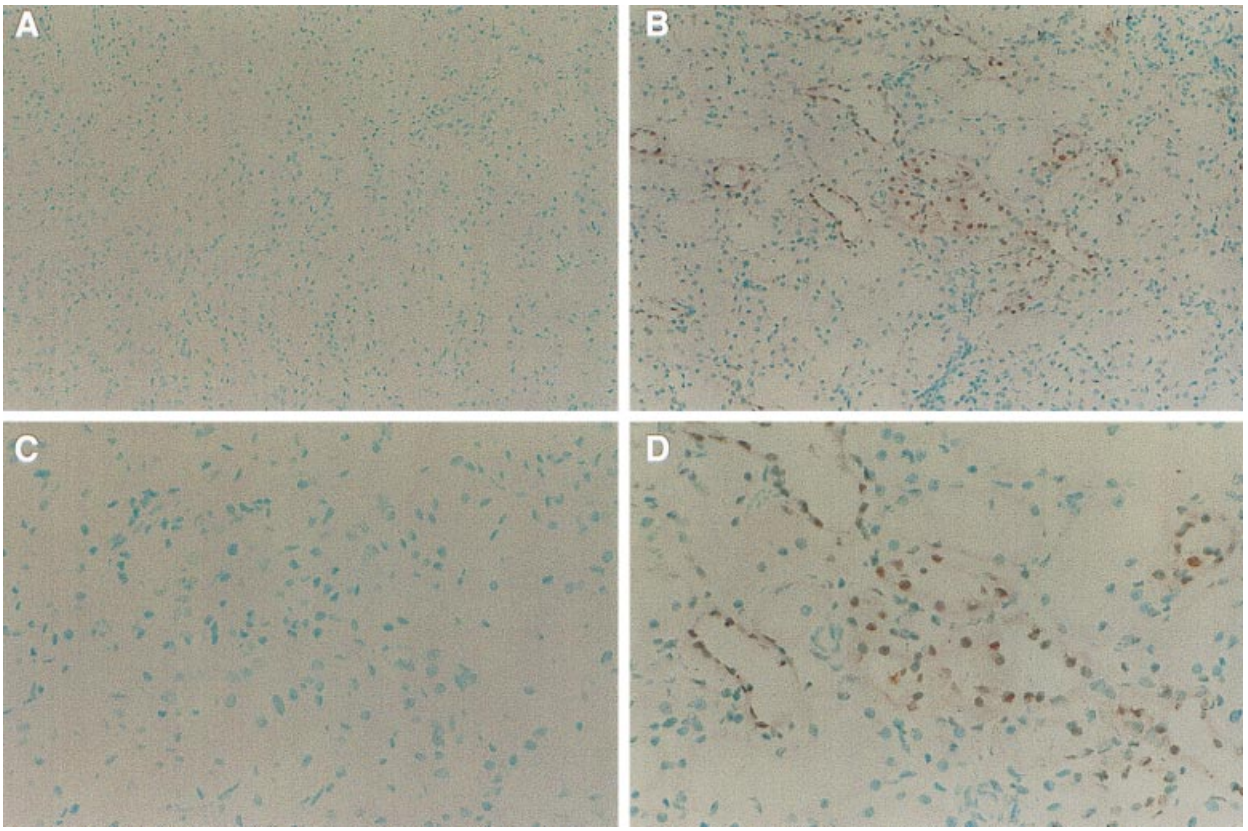

Fig. 11. Kidney sections studied by TUNEL assay. (*A*) Kidney sections from control rats examined at low power (×100) showing a lack of staining. (*B*) Kidney sections from rats with glycerol-induced acute renal failure studied three hours after glycerol at low power (×100) showing distal tubular profiles staining positively. (*C*) Kidney sections from control rats examined at high power (×200) again showing a lack of positivity. (*D*) Kidney sections from rats with glycerol-induced acute renal failure studied at three hours after glycerol at high power (×200) showing distal tubular profiles staining positively.

Table 2. Content of $8OHdG/10^5dG$ in the kidney in rats treated with sodium pyruvate or sodium chloride 3 hours after the administration of glycerol

	$8OHdG/10^5dG$
Sodium pyruvate, control ($N = 4$)	30 ± 7
Sodium pyruvate, glycerol ($N = 4$)	25 ± 2
Sodium chloride, control ($N = 4$)	22 ± 5
Sodium chloride, glycerol ($N = 4$)	39 ± 12

observed. However, 24 hours after the administration of glycerol, there was a significant increase in this marker of oxidative stress in the glycerol treated group (45.5 ± 5.6 vs. 61.9 ± 4.1, $P = 0.05$).

Using the TUNEL assay we observed DNA injury in kidneys three hours after the administration of hypertonic glycerol. These findings are shown in Figure 11. In untreated control rats ($N = 3$) there were rare, single cells in the kidney that stained positively (Fig. 11A, control, lower power; Fig. 11C, control, higher power). In contrast, in all rats studied three hours after the injection of hypertonic glycerol ($N = 3$), there was a significant number of distal tubules that stained positively (Fig. 11B, glycerol-treated kidney, lower power; Fig. 11D, glycerol-treated kidney, higher power). Such staining was observed in distal tubular epithelial cells and not in proximal tubules; once one cell in that profile stained positively, nearly all other cells in that profile were positive. Virtually identical findings were observed in all rats studied with glycerol-induced acute renal failure at six hours ($N = 3$ in each group). Similarly, clusters of TUNEL-positive tubules, again distal tubules, were also observed at 24 hours ($N = 3$ in each group).

We also sought to induce DNA injury by exposure of renal epithelial cells to heme at 10 and 50 μM. Since our *in vivo* studies demonstrated that the assay for DNA injury that was consistently positive at all time points was the TUNEL assay, we employed this assay in studies of DNA injury in cell lines that are proximally-derived ($LLC\text{-}PK_1$) and those that are distally-derived (MDCK). In control cells treated with buffer only, and in cells exposed to heme (10 μM) for three hours of exposure, no evidence of DNA injury by the TUNEL assay was observed either in $LLC\text{-}PK_1$ cells or MDCK cells. After exposure to heme (50 μM), some 20% of MDCK cells stained positively; such positivity was not observed in $LLC\text{-}PK_1$ cells.

Ultrastructural studies in the glycerol model

In light of findings observed in the TUNEL assay, we performed transmission electron microscopy on renal cortex and medulla isolated from glycerol-treated and control rats so as to define the morphologic mechanism of cell loss that occurs in this model. Additionally, such ultrastructural studies were needed to evaluate if structural derangements in mitochondria accompanied

the functional impairment we observed. Importantly, extensive evaluation of toluidine blue-stained survey sections failed to demonstrate morphologic evidence of apoptosis. Nuclear condensation, coarse clumping of nuclear chromatin, and cell swelling, which are features of necrosis rather than apoptosis, were observed in kidneys studied three hours after the administration of glycerol; these changes were more pronounced after 24 hours. Both proximal and distal tubules showed evidence of injury. Injured distal tubules were frequently associated with intratubular casts.

Regarding the mitochondrial compartment, we observed pronounced and progressive ultrastructural abnormalities in mitochondria, including swelling of the mitochondrial matrix and accumulation of amorphous matrix densities, the latter representing a marker of irreversible cell injury (Fig. 12). Interestingly, at three hours after the administration of glycerol, clusters of degenerate mitochondria, clearly identified by their cristae, were observed within membrane lined structures, findings that are consistent with the presence of autophagic vacuoles (Fig. 12 A, B). Breakdown and opacification of matrix structure were apparent after 24 hours injury (Fig. 12C). Thus, mitochondrial injury is quite prominent ultrastructurally as well as functionally in the glycerol model.

DISCUSSION

Within three hours of the induction of the glycerol model, we observed alterations in mitochondrial function as reflected by decrements in state 3 and uncoupled respiration. With glutamate and malate these changes were progressive such that at 24 hours there were marked decrements in states 2 and 3 respiration and uncoupled respiration. In the case of succinate/rotenone, state 3 and uncoupled respirations continued to decline at 24 hours whereas state 2 respiration was increased at 24 hours. We suggest that impairment in the electron chain between the entry of glutamate/malate and complex 1, at least in part, contributes to these effects.

These functional changes in mitochondria were accompanied by pronounced ultrastructural ones. While structural mitochondrial injury is described in prior studies in the glycerol model [27], certain arresting features we have observed, namely, autophagy of injured mitochondria, have not been reported in the glycerol model or, as far as we can glean from the literature, in other models of acute renal injury. Autophagy refers to a process by which cells first cordon off, and subsequently degrade, cytoplasmic contents and organelles including mitochondria [28, 29]. This process occurs in health and disease, in diverse tissues, and facilitates the containment, and ultimately, the removal of old and injured organelles [28, 29]. The finding of degenerate mitochondria in autophagic vacuoles three hours after the administration of glycerol underscores mitochondrial damage as a prominent feature in this form of acute renal injury.

To pursue the basis for mitochondrial dysfunction, we considered the involvement of intracellular heme which we reasoned would be markedly increased in the kidney exposed to heme proteins derived from muscle and erythrocytes. The premise that heme is toxic to the kidney is substantiated by experimental studies *in vivo* [30, 31] and by observations in patients [32]. In our prior studies [13], we noted that as early as three hours after the administration glycerol the heme-degrading enzyme, heme oxygenase, was induced, presumably reflecting increased intracellular heme [13]. Since heme is particularly injurious in the presence of hydrogen peroxide [33], we posited that mitochondria would be especially prone to such injury since this organelle generates hydrogen peroxide in the course of its normal metabolism [34]. Moreover, the lipid-enriched mitochondrial membranes would ensure the facile incorporation of heme, a lipophilic molecule, into mitochondria. We measured heme content in mitochondria and found such content to be increased some tenfold within three hours after the administration of glycerol. We then exposed intact mitochondria to heme concentrations that would permit such measurable levels of heme as those observed in the glycerol kidney. Such exposure to heme significantly altered oxygen consumption: mitochondria initially displayed increased respiration which gave way to a persistent decline in oxygen consumption until oxygen consumption was undetectable. Higher concentrations of heme shifted the curve to the left such that the early increase in oxygen consumption was blunted and the progressive decline in oxygen consumption was hastened. To explore the basis for these changes, we considered the possibility that oxidative stress imposed by heme would contribute to the early rise, and later decrement, in oxygen consumption. That oxidative stress was present in mitochondria was indicated by increments in TBARS, an index of malondialdehyde, which paralleled the increase in heme content. The administration of the antioxidant iron chelator, deferoxamine, prevented the early rise in oxygen consumption, thereby suggesting that this early increase in oxygen consumption was an oxidative, iron-dependent effect of heme. However, deferoxamine did not delay or mitigate the subsequent decline in oxygen consumption. This indicates that the subsequent decline in oxygen consumption can be dissociated from the early ion-dependent increase in mitochondrial respiration. We speculate that the early increase in oxygen consumption observed with heme is due to the appearance of the mitochondrial permeability transition [9]. This latter alteration is attended by increased porosity of mitochondrial membranes, the loss of mitochondrial transmembrane potential, uncoupling and increased respiration [9]. Since oxidants are recognized as a cause of the mitochondrial membrane transition [7, 15], we suggest that the early increase in respiration induced by heme may represent such iron-dependent oxidizing effects. We also suggest that the late decline in oxygen consumption may not be critically dependent upon iron *per se*, and may represent a direct toxic effect of the heme molecule itself rather than from iron. It is also possible that the iron chelator may not effectively chelate iron after heme has penetrated mitochondrial membranes.

We also assessed nuclear damage as a potential lesion in the glycerol model. We employed several indices since these multiple markers reflect distinct, yet complementary, aspects of DNA and cell injury. We failed to observe at either time point evidence of DNA laddering. At three hours we noted the appearance of TUNEL-positive cells in the distal nephron but not in the proximal nephron. At this time point we saw no structural evidence of apoptosis, nor did we see evidence of oxidative injury to DNA using the by 8-hydroxydeoxyguanosine index. At 24 hours, TUNEL-positive cells were still observed in abundance and this was now accompanied by the presence of increased amounts of 8-hydroxydeoxyguanosine, but not by structural evidence for nuclear injury as observed in apoptotic cell death. These findings underscore the nuanced manifestation of DNA injury in diseased states [10, 12, 21, 35], and they support the occurrence of

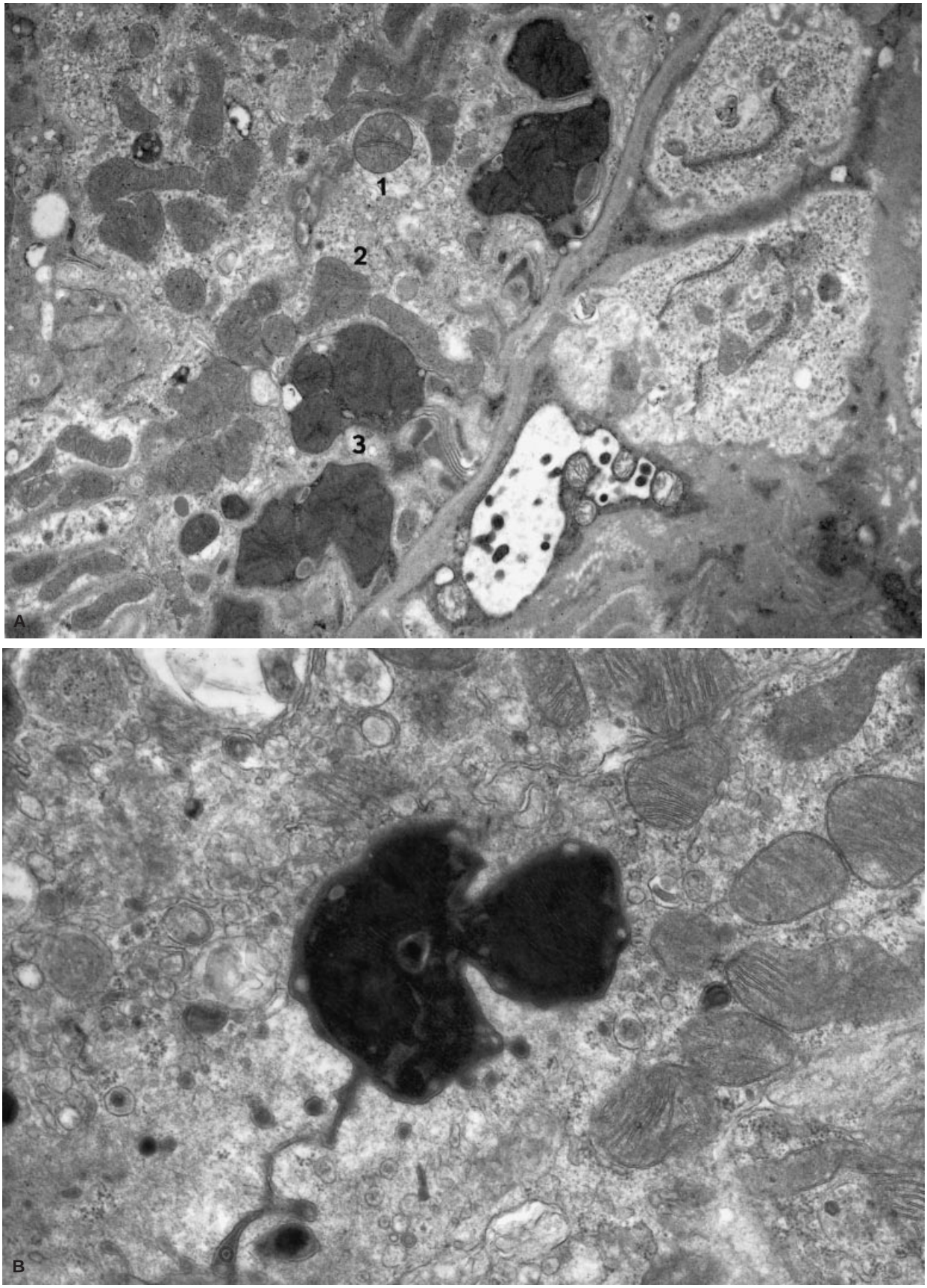

Fig. 12

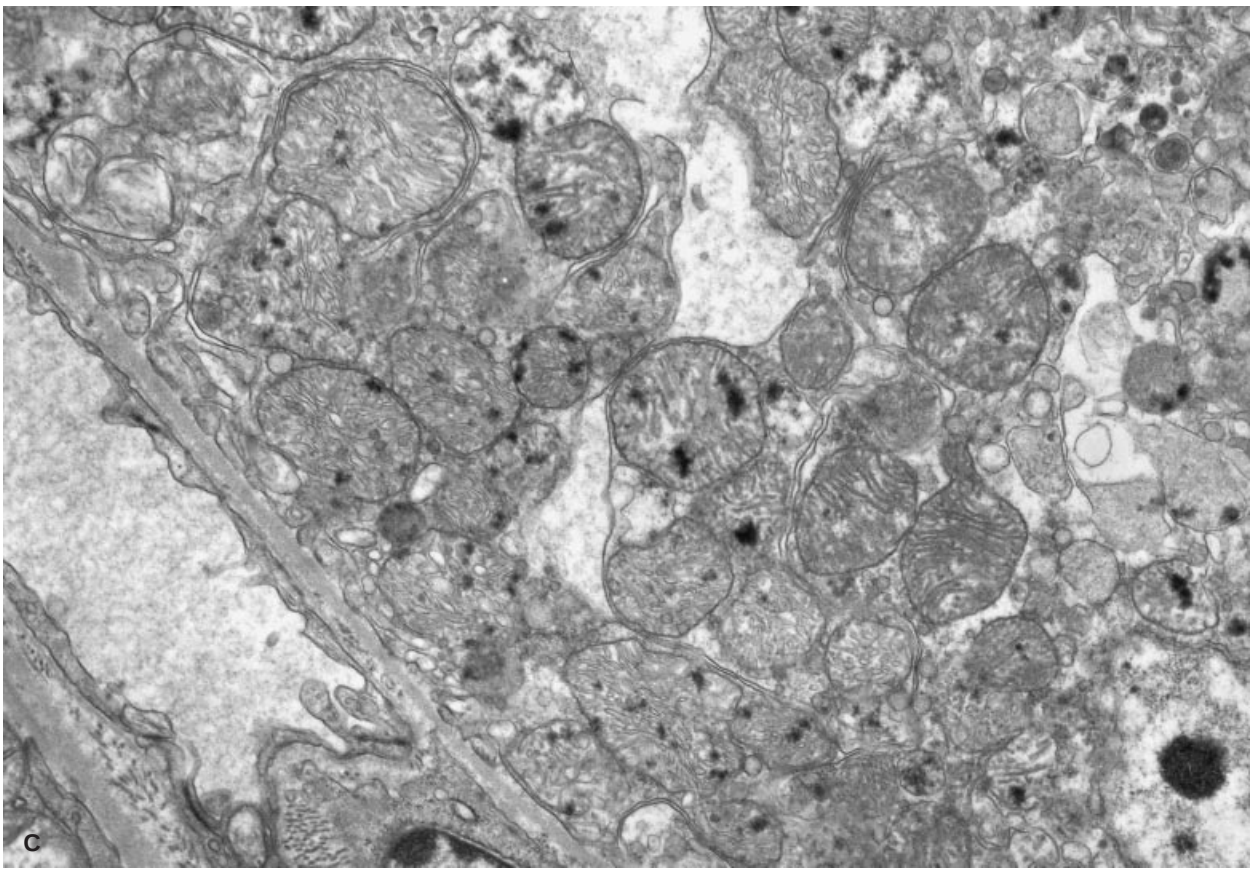

Fig. 12. ***Continued.***

Fig. 12. Electron microscopic studies in the glycerol model. (*A*) Mitochondria exhibiting stages of injury in kidneys harvested three hours after the administration of glycerol. Several populations of mitochondria are present including those that are swollen (1), those that exhibit loss of cristae (2), and those that are present in clusters within a membrane-lined vesicle representing an autophagic vacuole (3). (*B*) An autophagic vacuole containing degenerate mitochondria (identified in part by presence of cristae) in kidneys harvested three hours after administration of glycerol. Swollen mitochondria are present in surrounding regions. (*C*) Swollen mitochondria containing amorphous matrix densities, indicative of irreversible cell injury, in tubular epithelium from rat kidneys, 24 hours following glycerol exposure.

endonuclease activation without morphologic features of apoptosis [12]. The mechanisms underlying such endonuclease activation in the distal nephron await further study since the capacity of heme to evince such changes in distal nephron-derived cells, MDCK cells, while present in the minority of these cells at a higher dose of heme, clearly was not overwhelming, at least under the conditions studied.

Our studies assessing DNA injury *in vivo* indicate that the response of the distal nephron differs from the proximal nephron in this pathologic state, and is germane to the growing appreciation of site-specific response to injury along the nephron. These two parts of the nephron possess quite different metabolic characteristics: for example, the metabolic cost of sodium transport entails a higher rate of oxygen consumption in the distal nephron, the intermediary metabolism differs at these two sites while certain parts of the distal nephron are exposed to markedly lower ambient partial pressure of oxygen [36]. The vulnerability to oxidative stress as well as the antioxidant profile in these two regions are different [37, 38]. As illustrative of such differential behavior, it has been known for more than ten years that during autolysis, the distal nephron demonstrates morphologic features of apoptosis whereas the proximal nephron demonstrates features of necrosis [39]. DNA fragmentation and apoptotic changes occur in the thick ascending limb of rat kidneys in response to hypoxia, but are not seen in the proximal tubule [22]. A similarly selective effect is observed in contrast-induced acute renal injury [22]. Such DNA injury following ischemic/hypoxic injury is similar to the findings we observed in the glycerol model. In models of acute renal injury such as ischemia, there is a characteristic proliferative response that occurs in the proximal nephron following necrosis [40, 41]. On the other hand, the cells of the distal nephron demonstrate an immediate and prominent early gene response characterized by the expression of c-*fos*, c-*jun* and *EGF1*, but such cells do not progress through the cell cycle [40–43]. In cisplatin-induced nephrotoxicity, tubular necrosis is localized to the outer stripe of the outer medulla whereas the induction of clusterin, a putatively protective response, is found primarily in the inner stripe of the outer medulla [44]. Consistent with and germane to this theme are our present observations that the glycerol model exhibits a site-specific pattern of injury, namely, prominent endonuclease-dependent DNA injury in the distal but not proximal nephron.

The increments in heme we observed in mitochondria likely represent heme released from heme proteins that originate from injured muscle and erythrocytes. Such heme proteins are taken up and degraded by the lysosomal/endosomal system to release their heme moiety, which is then conveyed to the various organelles via the intracellular canulicular system [45, 46]. Additionally, intracellular heme proteins are plentiful in numerous cellular organelles including the mitochondria. It is possible that intracellular heme proteins are destabilized during conditions of oxidative stress, and as a consequence, release their heme moiety [24]. This paradigm, wherein an intracellular heme protein undergoes oxidative destabilization and releases its heme, is persuasively supported by studies in assorted forms of hemolysis [47, 48]. In such circumstances of oxidative stress, hemoglobin, located in the intracellular compartment in erythrocytes, is converted to methemoglobin and hemichromes, and ultimately provides free heme. Heme, released from a heme protein innate to the erythrocyte, in turn, attacks the cytoskeleton and lipid bilayer of erythrocytes–cells that lack nuclei and mitochondria–eventually causing lysis [47, 48]. Our studies, centered as they are on renal tubular epithelial cells, cells in which nuclei are present and mitochondria are abundant, uncover mitochondria and nuclei as potential targets for such injury in nucleated cells.

We conclude by speculating that our findings may be relevant not only to conditions of rhabdomyolysis and hemolysis but also to other forms of acute toxic injury in which organellar heme content is increased as occurs in cisplatin-induced nephropathy, and presumably results from the destabilization of intracellular heme proteins [24]. Our findings may also be relevant to hematuric glomerulopathies: based on the recognized phagocytosis and degradation of erythrocytes by renal tubules in hematuric conditions [49], the suggestion was raised previously that an attendant increase in cellular heme in such states may be toxic to tubules [50]. Interestingly, recent studies have called attention to the acute tubular damage in hematuric glomerulopathies that cannot be ascribed to glomerular structural changes or tubular obstruction [51]. We speculate that such cellular injury reflects, in part, heme-mediated organellar injury.

ACKNOWLEDGMENTS

These studies were supported by the following grants: DK47060 (K.A.N.) and HL55552 (K.A.N. and R.P.H.). An abstract of this work was presented at the 1996 Annual Meeting of the American Society of Nephrology and was published in abstract form (*J Am Soc Nephrol* 7:1843, 1996). We gratefully acknowledge the secretarial assistance provided by Mrs. Sharon Heppelmann.

Reprint requests to Karl A. Nath, M.B., Ch.B., Mayo Clinic, 200 First St., 542 Guggenheim Bldg., Rochester, Minnesota 55905, USA.
E-mail: nath.karl@mayo.edu

REFERENCES

1. Zager RA: Rhabdomyolysis and myohemoglobinuric acute renal failure. *Kidney Int* 49:314–316, 1996
2. Dubrow A, Flamenbaum W: Acute renal failure associated with myoglobinuria and hemoglobinuria (chapt 10), in *Acute Renal Failure* (2nd ed), edited by Brenner BM, Lazarus JM, New York, Churchill Livingstone, 1988, pp 279–294
3. Shah SV, Walker PD: Evidence suggesting a role for hydroxyl radical in glycerol-induced acute renal failure. *Am J Physiol* 255:F438–F443, 1988
4. Paller MS: Hemoglobin- and myoglobin-induced acute renal failure in rats: Role of iron in nephrotoxicity. *Am J Physiol* 255:F539–F544, 1988
5. Baliga R, Zhang Z, Baliga M, Shah SV: Evidence for cytochrome P-450 as a source of catalytic iron in myoglobinuric acute renal failure. *Kidney Int* 49:362–369, 1996
6. Weinberg JM, Harding PG, Humes HD: Mitochondrial bioenergetics during the initiation of mercuric chloride-induced renal injury. I. Direct effects of *in vitro* mercuric chloride on renal cortical mitochondrial function. *J Biol Chem* 257:60–67, 1982
7. Weinberg JM: The cellular basis of nephrotoxicity (chapt 39), in *Diseases of the Kidney* (5th ed, vol II), editited by Schrier RW, Gottschalk CW, Boston, Little, Brown and Company, Publishers, 1993, pp 1031–1098
8. Zager RA: Mitochondrial free radical production induces lipid peroxidation during myohemoglobinuria. *Kidney Int* 49:741–751, 1996
9. Kroemer G, Petit P, Zamzami N, Vayssière J-L, Mignotte B: The biochemistry of programmed cell death. *FASEB J* 9:1277–1287, 1995
10. Ueda N, Shah SV: Endonuclease-induced DNA damage and cell death in oxidant injury to renal tubular epithelial cells. *J Clin Invest* 90:2593–2597, 1992
11. Hagar H, Ueda N, Shah SV: Endonuclease induced DNA damage and cell death in chemical hypoxic injury to LLC-PK_1 cells. *Kidney Int* 49:355–361, 1996
12. Ueda N, Walker PD, Hsu S-M, Shah SV: Activation of a 15-kDa endonuclease in hypoxia/reoxygenation injury without morphologic features of apoptosis. *Proc Natl Acad Sci USA* 92:7202–7206, 1995
13. Nath KA, Balla G, Balla J, Jacob HS, Vercellotti GM, Levitt M, Rosenberg ME: Induction of heme oxygenase is a rapid protective response in rhabdomyolysis in the rat. *J Clin Invest* 90:267–270, 1992
14. Lemmi CAE, Pelikan PCD, Sikka SC, Hirschberg R, Geesaman B, Miller RL, Park KS, Liu SC, Koyle M, Rajfer J: Cyclosporine augments renal mitochondrial function in vivo and reduces renal blood flow. *Am J Physiol* 257:F837–F841, 1989
15. Nath KA, Croatt AJ, Likely S, Behrens TW, Warden D: Renal oxidant injury and oxidant response to mercury. *Kidney Int* 50:1032–1043, 1996
16. Floyd RA, Watson JJ, Wong PK, Altmiller DH, Rickard RC: Hydroxyl free radical adduct of deoxyguanosine: Sensitive detection and mechanisms of formation. *Free Rad Res Comms* 1:163–172, 1986
17. Enright HU, Miller WJ, Hebbel RP: Nucleosomal histone protects DNA from iron-mediated damage. *Nucl Acids Res* 20:3341–3346, 1992
18. Nath KA, Enright H, Nutter LM, Fischereder MF, Zou JN, Hebbel RP: The effect of pyruvate on oxidant injury to isolated and cellular DNA. *Kidney Int* 45:166–176, 1994
19. Enright H, Hebbel RP, Nath KA: Internucleosomal cleavage of DNA as the sole criterion for apoptosis may be artifactual. *J Lab Clin Med* 124:63–68, 1994
20. Gavrieli Y, Sherman Y, Ben-Sasson SA: Identification of programmed cell death *in situ* via specific labeling of nuclear DNA fragmentation. *J Cell Biol* 119:493–501, 1992
21. Zager RA, Fuerstenberg SM, Baehr PH, Myerson D, Torok-Storb B: An evaluation of antioxidant effects on recovery from postischemic acute renal failure. *J Am Soc Nephrol* 4:1588–1597, 1994
22. Beeri R, Symon Z, Brezis M, Ben-Sasson SA, Baehr PH, Rosen S, Zager RA: Rapid DNA fragmentation from hypoxia along the thick ascending limb of rat kidneys. *Kidney Int* 47:1806–1810, 1995
23. Nath KA, Balla J, Croatt A, Vercellotti GM: Heme protein-mediated renal injury: A protective role for 21-aminosteroids *in vitro* and *in vivo*. *Kidney Int* 47:592–602, 1995
24. Agarwal A, Balla J, Alam J, Croatt AJ, Nath KA: Induction of heme oxygenase in toxic renal injury: A protective role in cisplatin nephropathy in the rat. *Kidney Int* 48:1298–1307, 1995
25. McDowell EM, Trump BF: Histologic fixatives suitable for diagnostic light and electron microscopy. *Arch Pathol Lab Med* 100:405–414, 1976
26. Spurr AR: A low viscosity epoxy resin embedding medium for electron microscopy. *J Ultrastructural Res* 26:31–43, 1969
27. Preuss HG, Tourkantonis A, Hsu C-H, Shim PS, Barzyk P, Tio F, Schreiner GE: Early events in various forms of experimental acute necrosis in rats. *Lab Invest* 32:286–294, 1975

28. Glaumann H, Ericsson JL, Marzella L: Mechanism of intralysosomal degradation with special reference to autophagocytosis and heterocytosis of cell organelles. *Int Rev Cytol* 73:149–182, 1981
29. Brunk UT, Jones CB, Sohal RS: A novel hypothesis of lipofuscinogenesis and cellular aging based on interactions between oxidative stress and autophagocytosis. *Mutation Res* 275:395–403, 1992
30. Anderson WAD, Morrison DB, Williams EF Jr: Pathologic changes following injections of ferrihemate (hematin) in dogs. *Arch Pathol* 33:589–602, 1942
31. Corcoran AC, Page IH: Renal damage from ferroheme pigments myoglobin, hemoglobin, hematin. *Texas Reports Biol Med* 3:528–544, 1945
32. Jeelani Dhar G, Bossenmaier I, Cardinal R, Petryka ZJ, Watson CJ: Transitory renal failure following rapid administration of a relatively large amount of hematin in a patient with acute intermittent porphyria in clinical remission. *Acta Med Scand* 203:437–443, 1978
33. Balla G, Vercellotti GM, Muller-Eberhard U, Eaton J, Jacob HS: Exposure of endothelial cells to free heme potentiates damage mediated by granulocytes and toxic oxygen species. *Lab Invest* 64:648–655, 1991
34. Chance B, Sies H, Boveris A: Hydroperoxide metabolism in mammalian organs. *Physiol Rev* 59:527–605, 1979
35. Iwata M, Myerson D, Torok-Storb B, Zager RA: An evaluation of renal tubular DNA laddering in response to oxygen deprivation and oxidant injury. *J Am Soc Nephrol* 5:1307–1313, 1994
36. Gullans SR, Hebert SC: Metabolic basis of ion transport (chapt 5), in *The Kidney* (5th ed), edited by Brenner BM, Philadelphia, WB Saunders, 1997, pp 211–246
37. Andreoli SP, McAteer JA: Reactive oxygen molecule-mediated injury in endothelial and renal tubular epithelial cells in vitro. *Kidney Int* 38:785–794, 1990
38. Andreoli SP, Mallett C, McAteer JA, Williams LV: Antioxidant defense mechanisms of endothelial cells and renal tubular epithelial cells: role of the glutathione redox cycle and catalase. *Pediatr Res* 32:360–365, 1992
39. El-Shennaway IE, Gee DJ, Aparicio SR: Renal tubular epithelia ultrastructure in autolysis. *J Pathol* 147:13–21, 1985
40. Safirstein R: Gene expression in nephrotoxic and ischemic acute renal failure. *J Am Soc Nephrol* 4:1387–1395, 1994
41. Megyesi J, Di Mari J, Udvarhelyi N, Price PM, Safirstein RL: DNA synthesis is dissociated from the immediate-early gene response in the post-ischemic kidney. *Kidney Int* 48:1451–1458, 1995
42. Ouellette AJ, Malt RA, Sukhatme VP, Bonventre JV: Expression of two "immediate early" genes, *Egr-1* and *c-fos*, in response to renal ischemia and during compensatory renal hypertrophy in mice. *J Clin Invest* 85:766–771, 1990
43. Bonventre JV, Sukhatme VP, Bamberger M, Ouellette AJ, Brown D: Localization of the protein product of the immediate early growth response gene, *Egr-1*, in the kidney after ischemia and reperfusion. *Cell Regul* 2:251–260, 1991
44. Silkensen JR, Agarwal A, Nath KA, Manivel JC, Rosenberg ME: Temporal induction of clusterin in cisplatin nephrotoxicity. *J Am Soc Nephrol* 8:302–305, 1997
45. Bunn HF, Esham WT, Bull RW: The renal handling of hemoglobin. I. Glomerular filtration. *J Exp Med* 129:909–924, 1969
46. Bunn HF, Jandl JH: The renal handling of hemoglobin. II. Catabolism. *J Exp Med* 129:925–934, 1969
47. Hebbel RP, Eaton JW: Pathobiology of heme interaction with the erythrocyte membrane. *Semin Hematol* 26:136–149, 1989
48. Hebbel RP: The sickle erythrocyte in double jeopardy: Autoxidation and iron decompartmentalization. *Semin Hematol* 27:51–69, 1990
49. Hill PA, Davies DJ, Kincaid-Smith P, Ryan GB: Ultrastructural changes in renal tubules associated with glomerular bleeding. *Kidney Int* 36:992–997, 1989
50. Nath KA: Tubulo-interstitial disease as a major determinant of progressive renal injury. *Am J Kidney Dis* 20:1–17, 1992
51. Fogazzi GB, Imbasciati E, Moroni G, Scalia A, Mihatsch MJ, Ponticelli C: Reversible acute renal failure from gross haematuria due to glomerulonephritis: Not only in IgA nephropathy and not associated with intratubular obstruction. *Nephrol Dial Transplant* 10:624–629, 1995